Available online at www.sciencedirect.com

ScienceDirect

Energy Procedia 114 (2017) 4967 – 4974

Energy Procedia

13th International Conference on Greenhouse Gas Control Technologies, GHGT-13, 14-18 November 2016, Lausanne, Switzerland

Residual trapping of supercritical CO_2: direct pore-scale observation using a low cost pressure cell for micro computer tomography

Maxim Lebedev[a,c,*], Yihuai Zhang[b], Vassili Mikhaltsevitch[a,c], Stefan Inglauer[b], Taufiq Rahman[b]

[a]*Curtin University, Department of Exploration Geophysics, 26 Duck Perry Avenue, 6151, Perth, Australia*
[b]*Curtin University, Department of Petroleum Engineering, 26 Duck Perry Avenue, 6151, Perth, Australia*
[c]*CO2CRC, Australia*

Abstract

We describe the design and fabrication steps of a low-cost, modular experimental cell for flooding and X-ray tomography visualization of the rock samples at reservoir conditions (confining pressure up to 45 MPa, pore fluid pressure up to 20 MPa, and temperature up to 80°C). The main body of the cell is made from Polyether ether ketone (PEEK) tube. The cell can be easily machined and assembled in house from off-the-shelf components at a low cost. Modular design allows adopting the cell to a wide range of X-ray visualization experiments. To demonstrate the capabilities of the equipment we are presenting how the residual CO_2 phase spreads in the rock as a function of thermo-physical conditions, namely, for ambient condition CO_2 gas, near-critical CO_2 gas, liquid CO_2, and supercritical CO_2.

Peer-review under responsibility of the organizing committee of GHGT-13.

Keywords: CO2, rocks, micro CT, pressure cell

* Corresponding author. Tel.: +61-8-9266-2330; fax: +61-8-9266-4979.
E-mail address: m.lebedev@curtin.edu.au

Peer-review under responsibility of the organizing committee of GHGT-13.
doi:10.1016/j.egypro.2017.03.1639

1. Introduction

Injection of CO_2 into the subsurface is one of the known methods to mitigate greenhouse gas emissions [1-3]. The buoyant CO_2 is contained in the subsurface by structural, residual, dissolution and mineral trapping mechanisms. Quantitative knowledge of the residual trapping capacity of the reservoir is thus crucial for storage site selection. This residual saturation depends on porosity, initial CO_2 saturation, pore morphology and wettability, or in other words on reservoir properties at the microscopic level; note that the macroscopic residual saturation also depends on sweep efficiency and gravity. Therefore, it is of crucial importance to understanding the major factors, which determine residual trapping efficiency. Micro-CT tomography technique is a powerful tool to understand such factors at micro-level.

It is standard practice in micro-CT to image rocks at ambient conditions (i.e. at room pressure and temperature) [4-5]. However, reservoir rocks are buried at such depth that they experience high stresses and temperatures. The thermodynamic properties of the fluids inside the reservoir are pressure and temperature dependent. Therefore, transport properties are also temperature and pressure dependent. Moreover, it is well established that elastic rock properties of rocks are strongly affected by stress and or fluid distribution. Thus in order to acquire realistic pore network structures and fluid distributions (including but not limited to residual saturation), and to reliably estimate transport and elastic properties from micro images, rocks have to be imaged at reservoir pressure and temperature conditions. At this moment, cells for micro-CT are custom made [6-7] and thus are expensive.

We thus have developed suit of X-ray transparent pressure and temperature (P-T) cells capable of holding from 5 mm to 38.5 mm diameter samples. To demonstrate capabilities of the equipment, in this paper we report how the residual CO_2 saturation depends on the thermodynamical conditions of the CO2 (which changes from gas to liquid, near-supercritical and supercritical), in order to link CO_2 saturation and fluid distribution to acoustic properties of the samples.

2. Pressure cells for microCT

We have designed and fabricated two X-ray transparent pressure – temperature cell: both cells are utilized for visualization of the process inside the reservoir samples during flooding. The first cell is prepared for the simultaneous acoustic measurements and CT imaging at moderate resolution (40 um) of the 38.5 mm (1.5”) in diameter samples; the second one is applied for micro-CT imaging of smaller samples (5mm in diameter) at sub-micrometer resolution. Cell for big samples is shown in Fig. 1(a), this cell has been described in details previously [8-9].

Fig.1 (b) shows the cell for high-resolution imaging. This cell can be easily fabricated and assembled from off-the-shelf components at a low cost. Modular design allows adaptation of the cell to a wide range of X-ray experiments. The main body of the pressure cell is made from a 21-mm-diameter, 300-mm-long PEEK (Polyether ether ketone) rod supplied by RS components. A 8 mm in diameter hole to accommodate the sample inside was drilled in the laboratories’ workshop using a lathe. All other parts of the cell have been assembled from the standard Swagelok fittings. Both ends of the cell have the same assembly. Stainless steel, ¾” nuts with ferrule are swaged on both ends of the PEEK tube. The ¾” to ¼” unions are connected to both ends of the PEEK rod. The ¼” tees unions fittings are using for confining pressure supply and getting through of two 1/8 ” stainless steel fluid lines inside the cell. The cell is fixed on the rigid holder that can be easily connected to a stage inside micro-computed tomography (μCT). A 5-mm-diameter sample was jacketed in the rubber sleeve and was connected to the fluid lines using custom made plastic platens. Some steps of the fabrication and assembly and testing of the cell are shown in Fig. 2.

The arrangement of the cell inside X-ray micro-CT (3D X-ray Microscope VersaXRM 500 (XRadia-Zeiss) is shown in the Fig. 3. X-Y-Z micropositioning stage of the X-ray micro-CT is able to hold up to 10 kg weight; the weight of the developed cells is not exceed kg, thus the pressure cell with can be fixed to X-Y-Z stage without compromising performance of the scanner. All hydraulic and fluid lines of the cell are connected to equipment by flexible PEEK 1/8" tubes (Sigma-Aldrich). Such flexible tubes allows the rotation of the cell from -180° to +180° during the imaging. Confining pressure to a sample is applied by a set of syringe pumps (Teledyne-Isco 260 and 500 series). Depending on the requirements of the experiment, the heating and cooling of the sample inside the cell can be done by using continuous circulating of the pressurized confining fluid. A small flexible electrical heater attached to the low part of the cell (not shown in the Figures) can be used to boost the heating process. Injection of the fluids into the sample is performed using two syringe pumps (Teledyne-Isco 100 and 260 series). All pumps are placed in a outside X-ray micro-CT. All pumps and connecting tubes are maintained at a given temperature within the range -15°C +80°C by circulating of liquid antifreeze.

.

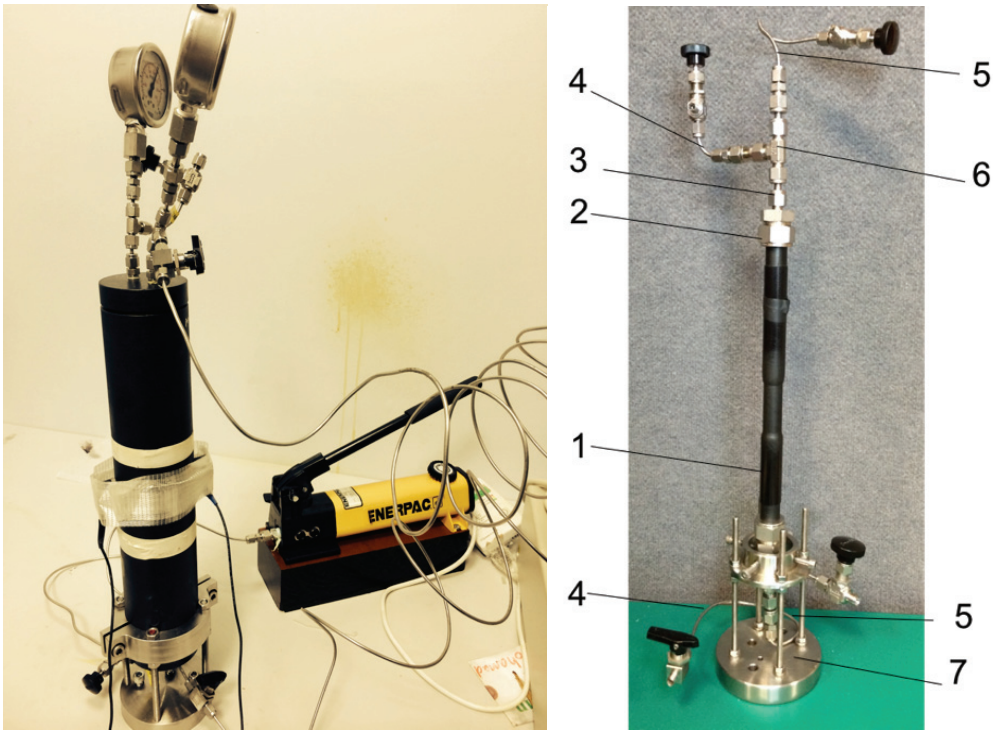

Fig. 1. Pressure-Temperature cells for CT: a) pressure cell for 5 mm diameter samples; b) pressure cell for 38.5 mm diameter samples: 1) – PEEK pipe; 2) Stainless steel, ¾" nuts with ferrule; 3) ¾" to ¼" unions; 4) confining pressure line 1/8"; 5) pore pressure/ flooding line; 6) ¼" tees union; 7) stage to be fixed to X-Y-Z stage of the micro-CT. .

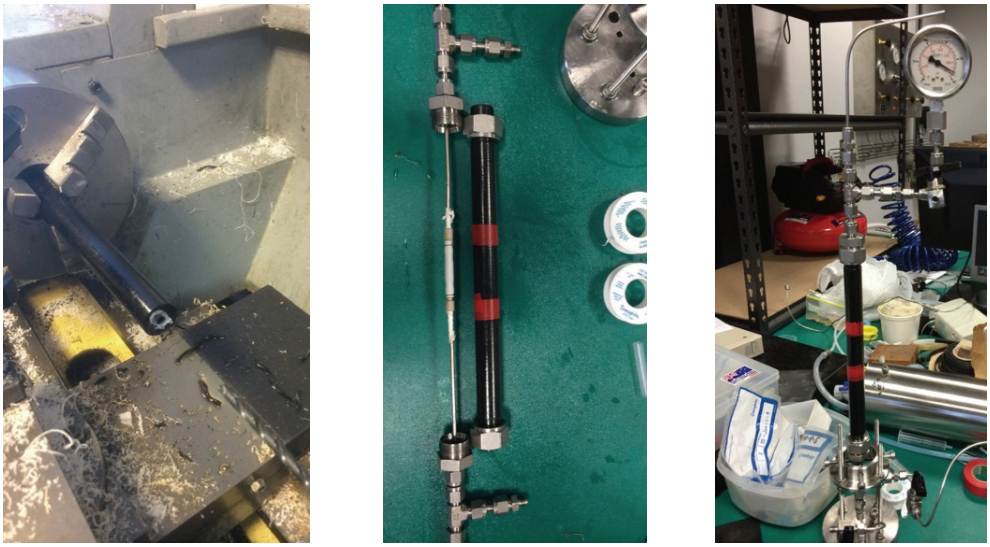

(a) **(b)** **(c)**

Fig. 2. (a) Fabrication of the PEEK tube in the lab; (b) cell assembly: sample inside the white rubber sleeve is connected to flooding lines; (c) hydraulic test outside the micro-CT (confining pressure is 33 MPa, zero pore pressure);

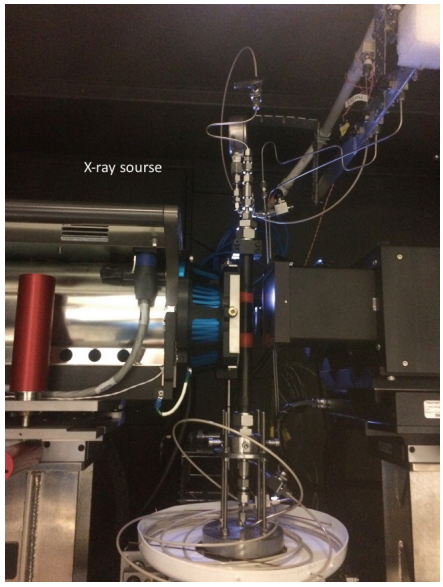

Fig. 3. Pressure - Temperature cell inside micro-CY. X-Ray source in on the left, X-Ray objective (detector) is on the right.

3. Demonstration experiments.

The cylindrical sample has been drilled from the bigger block, the sample is trimmed to size to accommodate inside a rubber sleeve inside the cell. After pressure test outside, the cell is placed inside micro-CT and the test image is performed. The cell and all hydraulic systems inside and outside the micro-CT are heated to designated temperature and controlled within 0.5C accuracy.

Monitoring and control of fluid injection inside the sample are performed between high-resolution imaging. Such real time in situ flooding visualization technique allows to estimate the amount of pore volumes (PV) injected inside the sample more precisely. Fig. 4 shows the sequence of X-ray radiographs, i.e. one plane projection, of the Bentheimer sandstone sample inside the cell acquired at 20 MPa of confining pressure. Radiograph (a) is taken for the dry sample. On the radiograph (b) it can be observed that brine (doped with ten present of sodium iodate) is entering the sample from the bottom and coming out the sample from the top. The last image (c) is the image after liquid CO_2 injection at 10 MPa injection pressure.

At each stage of the experiment, 3D imaging of the sample is performing at X-Ray energy ranged from 40kV to 80kV. Minimum time to acquire one 3D image is about 1.5h. During the acquisition the injection valve is closed thus no fluid is injecting into the sample. However, the backpressure is maintained by a production pump. Fig. 5 shows 2D images (sliced from 3D) of the dry, brine saturated and after liquid CO_2 flooding Bentheimer sandstone acquired at confining pressure of 20 MPa, pore pressure of 10 MPa, and temperature of 28°C with a nominal voxels size resolution of $(3.4348\mu m)^3$.

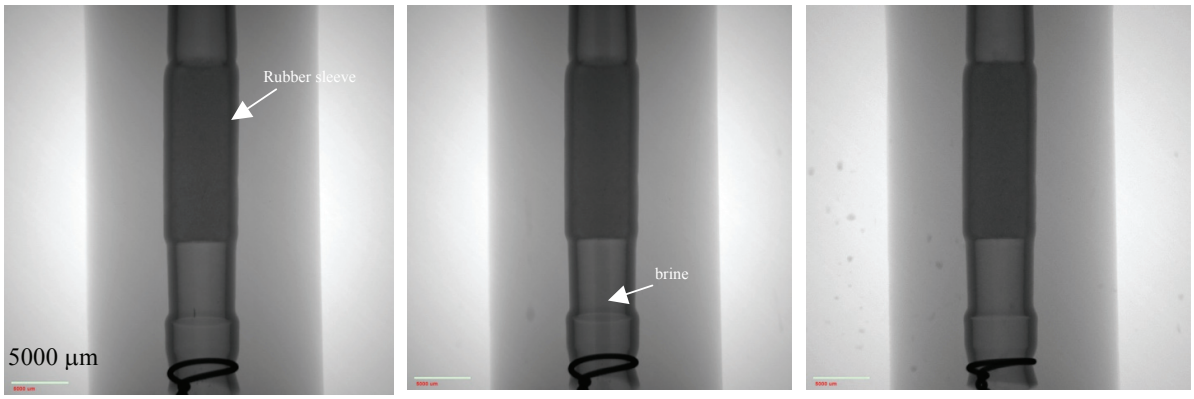

Fig. 4. Time lapse of X-ray radiographs of the sample inside the cell at 20 MPa confining pressure: (a) dry sample; (b) brine injection; (c) after CO2 injection. Low resolution image using 0.4x objective.

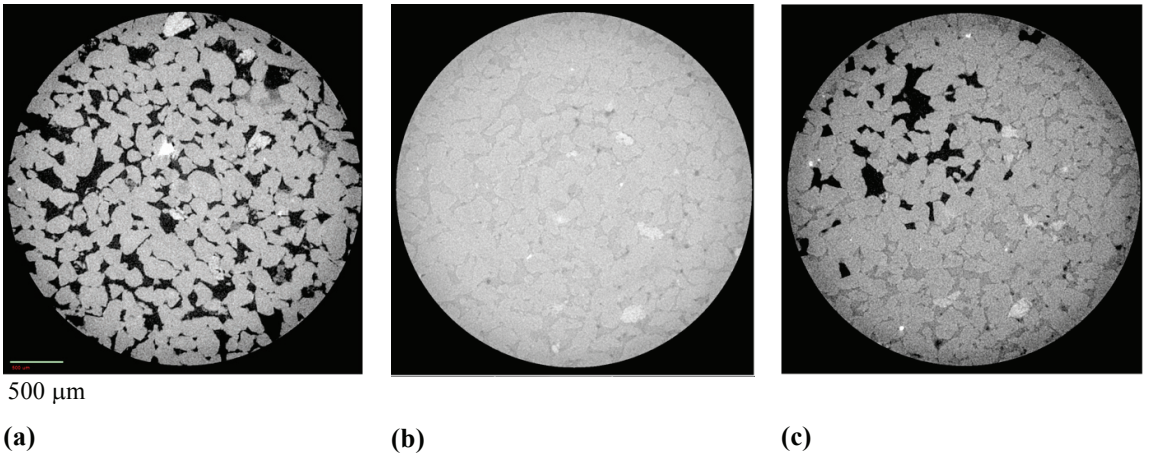

Fig. 5. Tomographic images in the flooding experiment. (a) dry sample; (b) 10%NaI-doped brine saturated sample; (c) after flooding with liquid CO_2. The direction of CO_2 injection is perpendicular to the paper plane. X-ray energy is 80kV, the distance between X-Ray source and the sample is 20 mm, the distance between the sample and 4x objective is 20 mm; pixel size is 3.4348 micrometer. Confining pressure is 20 MPa, pore pressure is 10 MPa, the temperature is 28°C. Note that the images (b) and (c) are corresponding to the same area of the sample.

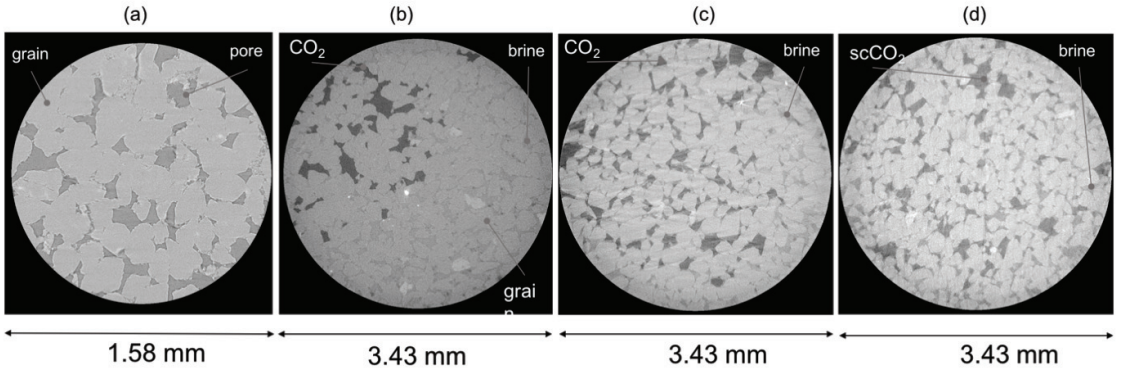

Fig. 6. Influence of Pressure, Temperature and Fluid on the image quality. Bernheimer sandstone, gas permeability 1880mD. X-Ray energy is 60kV, the distance between X-Ray source and the sample is 19 mm, the distance between the sample and 4x objective is 19 mm; pixel size is 3.4348 micrometer. Number of scans (radiographs) is 4001: (a) Dry sample, Pconf=30 MPa, T=28°C; (b) after liquid CO_2 injection into brine saturated sample, Pconf=25 MPa, Ping=10 MPa, T=28°C; (c) after "near critical" CO_2 injection into brine saturated sample Pconf=15 MPa, Ping=7 MPa, T=42°C; (d) after supercritical-CO_2 injection into brine saturated sample Pconf=15 MPa, Ping=10 MPa, T=42°C.

By increasing the pressure and especially temperature during the experiment the quality of raw images can decrease. Such slight degradation in quality caused mainly by the sample drift induced by a circulating high pressure and temperature confining fluid. Fig. 6 shows how raw image quality changes when pressure and temperature increases.

.

4. Conclusion

The simple experimental cells that allow microtomographic visualization of fluids inside rocks under elevated pressure was presented. The modular cell design allows hassle-free maintenance and easily modifications of the cell. The cell can be used for visualisation of multiphase fluids distribution inside porous media.

Using developed cell, we investigated how the residual CO_2 phase spreads in the rock as a function of thermo-physical conditions (for ambient condition CO_2 gas, liquid CO_2, near-critical CO_2 gas, and supercritical CO_2); and how residual CO_2 is dissolved by undersaturated formation brine (dissolution trapping). We found that CO_2 spread is relativelyhomogeneous throughout the core plugs for all conditions; however, less $scCO_2$ was trapped at higher pressures, which is possible due to the lower water-wettability of sandstone at high pressures. We conclude that μCT is a very powerful tool for non-destructive visualisation of microstructure as well as pore-scale fluid distribution inside rocks samples.

So far the micro-CT cell has been successfully used in the following experiments pressure research [10-14].

Acknowledgements

The author would like to thank the National Geosequestration Laboratory (NGL) for providing access to the X-ray microscope VersaXRM-500 (XRadia-Zeiss Ltd).

References

[1] Lackner, KS. Climate change. A guide to CO2 sequestration. Science 2003;300:1677–1678.

[2] Intergovernmental Panel on Climate Change (IPCC), IPCC special report on carbon dioxide capture and storage, prepared by Working Group III of the Intergovernmental Panel on Climate Change, Cambridge University Press, 2005.

[3] F.M. Orr, F.M. Onshore geologic storage of CO2. Science 2009;325:1656–1658.

[4] Madonna C., Quintal B., Frehner M., Almqvist BSG., Tisato N., Pistone M., Marone F. Saenger EH. Synchrotron-based X-ray tomographic microscopy for rock microstructure investigations. Geophysics 2013;78: D53-D64.

[5] Shulakova, V., Pervukhina, M., Müller, M., Lebedev, M., Mayo, S., Schmid, S., Golodoniuc, P., De Paula, O.P., Clennell, M.B., Gurevich, B. Computational elastic up-scaling of sandstone on the basis of X-ray micro-tomographic images. Geophysical Prospecting 2013;61:287-301.

[6] Iglauer, S., Paluszny, A., Pentland,CH., Blunt, MJ. Residual CO2 imaged with Xray micro-tomography. Geophysical Research Letters 2001;38:L21403.

[7] Fusseis, F., Steeb, H., Xiao, X., Zhu, W., Butler, I., Elphicka, S., Mader , U. A low-cost X-ray-transparent experimental cell for synchrotron-based X- ray microtomography studies under geological reservoir conditions. Journal of Synchrotron Radiation 2014; 21: 251-253.

[8] Lopes, S., Lebedev, M., Mueller, T., Clennell, B., Gurevich, B. Forced imbibition into a limestone: measuring P-wave velocity and water saturation dependence on injection rate. Geophysical Prospecting 2014;62: 1126-1142.

[9] Lebedev, M., Iglauer, S., Mikhaltsevitch, V. Acoustic Response of Reservoir Sandstones during Injection of Supercritical CO2. Energy Procedia 2014;63:4281-4288.

[10] Rahman, T., Lebedev, M., Barifcani, A., Iglauer, S. Residual trapping of supercritical CO2 in oil-wet sandstone. Journal of Colloid & Interface Science 2016; 469:63–68.

[11] Saenger, EH., Lebedev, M., Uribe, D., Osorno, M., Vialle, S., Duda, M., Inglauer, S., Steeb, H. Analysis of high resolution X-ray CT images

of Bentheim Sandstone under elevated confining pressures. Geophysical prospecting 2016;64:848-859.

[12] Zhang, Y., Xu, X., Lebedev, M., Sarmadivaleh, M., Barifcani, A., Iglauer, S. Multi-scale x-ray computed tomography analysis of coal microstructure and permeability changes as a function of effective stress. International Journal of Coal Geology 2016;165:149-156

[13] Zhang, Y., Lebedev, M., Sarmadivaleh, M., Barifcani, A., Iglauer, S. Swelling-induced changes in coal microstructure due to supercritical CO2 injection. Geophysical Research Letters 2016;43: doi:10.1002/2016GL070654

[14] Zhang, Y., Lebedev, M., Sarmadivaleh, M., Barifcani, A., Rahman , T., Iglauer, S. Swelling effect on coal micro structure and associated permeability reduction. Fuel 2016;182:568-576.